

Divertor retention for recycling impurities

To cite this article: J. Roth *et al* 1992 *Nucl. Fusion* **32** 1835

View the [article online](#) for updates and enhancements.

You may also like

- [SOLPS analysis of changes in the main SOL of DIII-D associated with divertor detachment vs attachment and closure vs openness](#)
C.F. Sang, H.Y. Guo, P.C. Stangeby et al.
- [Plasma detachment in divertor tokamaks](#)
A W Leonard
- [Performance assessment of long-legged tightly-baffled divertor geometries in the ARC reactor concept](#)
M.R.K. Wigram, B. LaBombard, M.V. Umansky et al.

DIVERTOR RETENTION FOR RECYCLING IMPURITIES

J. ROTH, K. KRIEGER, G. FUSSMANN

Max-Planck-Institut für Plasmaphysik,
Euratom-IPP Association,
Garching/Munich, Germany

ABSTRACT. A quick and simple experimental method of comparing the global retention capabilities of different divertor configurations for gaseous impurities is presented. Short gas puffs into the main chamber and analysis of the time dependence of central impurity lines are used to determine the retention capability in terms of time constants, which characterize the impurity leakage rate from the divertor chamber to the main plasma and to the pumping system. A simple two-reservoir model is used to define these basic parameters of divertor retention. For a more detailed evaluation of the divertor retention parameters from spectroscopic data, an impurity transport code is used to simulate the impurity radiation measured in various experiments. The dependence of the retention capability on the divertor plasma density and temperature as well as on the distance along the field lines back to the main plasma is discussed. The dependence on the impurity species is also investigated. On the basis of these results, the consequences of the divertor retention for helium exhaust in future fusion devices are analysed by numerical simulation.

1. INTRODUCTION

Thermonuclear fusion experiments such as JET [1] have reached plasma parameters which result in power amplification factors Q of about 1 for the prospective use of D-T as working gas. One limiting factor is the plasma dilution by light impurities from the wall such as C or Be [2] and also by estimated concentrations of He from fusion particles [3, 4]. Though the central He concentrations are ultimately given by the central α -particle confinement, this concentration may further increase owing to He recycling from the vessel walls and insufficient pumping capacity. Therefore, the retention of gaseous impurities in divertors and pumped limiter structures and their removal by external pumps attracts increasing interest [5–11]. Since these wall structures will also be the main source of sputtered impurity atoms, divertor retention of non-recycling impurities is an important issue too [12].

Impurity transport along the plasma scrape-off layer to the divertor has been extensively studied for the closed divertor geometry of ASDEX using multifluid codes [13, 14]. It could be shown that, for typical ASDEX conditions, the impurity transport from the divertor to the main plasma is predominantly ionic rather than neutral. The condition for higher divertor retention was found to be a high local Mach number of the background hydrogen ions. For low Mach numbers, thermal forces, directed towards the high temperature edge plasma, slow down or even reverse the impurity flow. Further studies using 2-D fluid codes [15, 16] including profile effects in the boundary

and the divertor showed a complicated impurity flow pattern. For high divertor recycling and low Mach number, highly ionized impurities diffusing out of the main plasma are practically confined to the main chamber by thermal forces. Neutral impurities originating from the main chamber walls are ionized in the plasma edge region, and only a few per cent of them finally enter the divertor owing to backward thermal forces. Target produced neutral atoms, however, are ionized and mostly swept back immediately to the target [17]. A comparison of these findings with Ar and Cu retention experiments in ASDEX shows qualitative agreement with the observed decrease of the retention at low density and increasing neutral beam injection (NBI) power. However, a quantitative match to the dramatic breakdown of the divertor retention with increasing NBI power could not be obtained. The fluid model may not be applicable under these conditions of low densities and long mean free paths of plasma and impurity ions. Kinetic codes indicate a complicated flow pattern, but published results for different divertor geometries are scarce [18, 19].

Since for a detailed understanding of impurity transport in a given divertor structure 2-D fluid or kinetic codes will be required, a quick and simple experimental method to compare the global retention capability of different divertor configurations is needed. Short puffs of inert gases into the main plasma and observation of line intensities in the main plasma and divertor are often used [5–11, 20] and allow the extraction of global divertor retention times. To compare different geometries, a simple two-reservoir model is presented

in this paper. Analytic solutions for time dependent impurity concentrations in the main plasma and in the divertor will be compared with experimental results in ASDEX [5, 6]. The dependence of the retention capability on the divertor plasma density and temperature as well as on the distance along field lines back to the main plasma will be pointed out. For a comparison with other experiments, such as JET [7, 8], DIII-D [9] and TEXTOR [10, 11], the 1-D impurity transport code ZEDIFF [21] has been used to take into account temporal changes of the central plasma and of plasma boundary parameters during auxiliary heating periods. This will make it possible to compare the widely different structures of plasma-wall contact and pumping in these machines as well as to point out important divertor properties for future machines.

2. THEORETICAL CALCULATIONS

2.1. Two-chamber model

As the knowledge of transport processes in the divertor is still limited and results from 2-D calculations [22, 23] reproduce experimental data only qualitatively, we introduce here a simple two-chamber model for a comparison of different divertor geometries (Fig. 1).

The confined plasma with a total number of impurity ions N_+ loses a flux of ions Φ_+ into the divertor chamber in accordance with a plasma confinement time τ_p . This time constant reflects the loss rate $-N_+/\tau_p$ of a decaying plasma without sources. In the case of a constant diffusion coefficient D and an inward flow velocity v_{in} , increasing proportionally to the minor radius, the confinement time can be estimated as $\tau_p \approx 0.173 \exp(0.17 v_{in} a / D) a^2 / D$ [24], with a being the plasma radius. Although the loss rate is actually obtained by integrating the outgoing flux density over the plasma surface (separatrix), it appears in this global treatment as a volume averaged sink term,

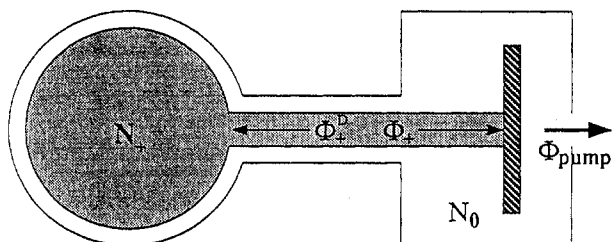


FIG. 1. Schematic view of the two-chamber divertor model.

with τ_p being the mean confinement time for a peaked impurity density distribution (e.g. the Bessel function $J_0(2.41r/a)$ for the case $v_{in} = 0$).

The outflowing ions are neutralized at the divertor plates and set up a neutral density in the divertor chamber with a total particle number N_0 . The neutral atoms are pumped out of this region with a characteristic time constant τ_{pump} . In addition, there is a refuelling flux Φ_0 out of the divertor and back into the main plasma chamber, providing there a particle source N_0/τ_D in the edge region (τ_D being the mean residence time of a particle in the divertor without external pumping). However, in order to be consistent with the sink term, this edge source is to be multiplied by a factor $\gamma < 1$ to convert it into an equivalent core source (i.e. postulating the same radial particle distribution for the sink term and the source term).

The quantities τ_p and γ can be obtained from a time dependent 1-D computer code in the following way: First, the particle confinement time (decay time) is obtained by switching off the impurity sources. After a short time interval, $\Delta t < \tau_p$, the profiles factorize into an exponential time behaviour and a radial eigenfunction $n_+(r, t) = f(r) \exp(-t/\tau_p)$, i.e. the impurity density decays without change of the radial distribution. Thus, for non-recycling impurities the total particle number N_+ will also decay exponentially with the time constant τ_p . This decay time constant τ_p is measured in the same way in laser blow-off experiments. In a second step, the factor γ can be determined from the analysis of a stationary situation, $dN_+/dt = -N_+/\tau_p + \gamma Q_{edge} = 0$, as

$$\gamma = N_+ / (\tau_p Q_{edge}) \quad (1)$$

where $Q_{edge} = \int q_{edge}(r) dV$ is the volume integrated source strength for a specified source density $q_{edge}(r)$.

Finally, in the case of fusion produced helium, there is an additional core source Q_+ . The confinement time τ_+ of ions created in a narrow source region in the plasma centre will be slightly larger than τ_p and is given by $\tau_+ = \gamma_{core} \tau_p$, where γ_{core} can be computed in the same way as γ . However, γ_{core} is usually close to 1 (e.g. ≤ 1.3 for both He and Ar), whereas, in contrast, γ can become appreciably smaller than unity. Therefore, we assume in the following $\tau_+ \approx \tau_p$.

The sink term describing the pumping losses, $S_{pump} = -N_0/\tau_{pump}$, has been omitted in an earlier analytical evaluation of Ar and Ne pulse experiments [20], but it proves to be important because τ_{pump} is, at least for ASDEX and DIII-D, of the same order of magnitude as τ_D/γ .

When all terms are taken into account, the following two coupled differential equations are obtained:

$$\frac{dN_+}{dt} = -\frac{N_+}{\tau_p} + \gamma \frac{N_0}{\tau_D} + Q_+ \quad (2)$$

$$\frac{dN_0}{dt} = +\frac{N_+}{\tau_p} - \gamma \frac{N_0}{\tau_D} - \frac{N_0}{\tau_{\text{pump}}} \quad (3)$$

Interpreting the measurements on the basis of these equations, the three quantities τ_p , τ_{pump} and τ_D/γ can be determined. Hence, to obtain the actual divertor time constant τ_D , an additional knowledge of the reduction factor γ is indispensable.

The model outlined so far is directly applicable to the case where plasma refuelling is caused by a flux of neutrals leaking out of the divertor. In this case the source distribution $q_{\text{edge}}(r)$ is determined by the penetration depth of the neutrals. Typically, the maximum of this function for noble gases at room temperature is a few centimetres outside the separatrix, resulting in rather small values of γ (e.g. ≈ 0.25 for He and ≈ 0.08 for Ar). On the other hand, as will be shown in Section 4, in ASDEX the neutrals have an extremely small probability to reach the main plasma because of ionization in the divertor slits (bypass ducts being negligible). To explain our observations, which clearly show refuelling from the divertor (i.e. a source term proportional to N_0), we have to assume that particles that are ionized in the divertor can reach the main plasma. These particles impose an edge source distribution which we assume to be localized close to the separatrix. Our model thus applies to this case as well, and the only difference from the above mentioned neutral refuelling is a different reduction factor γ_+ . Assuming a δ -function-like source distribution at the separatrix, γ_+ is found to be approximately 0.23 for both He and Ar.

2.1.1. Steady state solution

In the case of external pumping, steady state conditions can only be obtained if there is a constant impurity source Q_+ . If the impurities are created in the very plasma centre owing to fusion reactions, their confinement time $\tau_+ \approx \tau_p$, as mentioned above, will be different from the global ion confinement time $\gamma\tau_p$ which applies for impurities entering the plasma from the edge. Thus we obtain from Eq. (2)

$$N_+ = \left(\gamma \frac{N_0}{\tau_D} + Q_+ \right) \tau_p \quad (4)$$

In steady state it is required that

$$Q_+ = \frac{N_0}{\tau_{\text{pump}}} \quad (5)$$

Thus, the impurity content is obtained as

$$N_+ = Q_+ \tau_p \left(1 + \gamma \frac{\tau_{\text{pump}}}{\tau_D} \right) \quad (6)$$

Under these stationary conditions, the ratio of the number of impurity ions in the main plasma to those in the divertor chamber is

$$\frac{N_+}{N_0} = \tau_p \left(\frac{1}{\tau_{\text{pump}}} + \frac{\gamma}{\tau_D} \right) \quad (7)$$

From these equations, one sees immediately that good boundary screening, i.e. a small value of γ , or good divertor retention, i.e. a large value of τ_D , will decouple the main plasma content from the neutral content in the divertor in such a way that both quantities are proportional to the central confinement time ($N_+ \approx Q_+ \tau_p$) and the pumping time ($N_0 \approx Q_+ \tau_{\text{pump}}$) [3].

2.1.2. Time dependent solution

If the plasma particle confinement time τ_p is known, for example from laser blow-off experiments for non-recycling impurities, the time constants τ_{pump} and τ_D/γ can be determined from the decay of the impurity content N_+ after switching off a gas valve or after a short external gas puff. In this case, the coupled equations (2) and (3) have to be solved with $Q_+ = 0$.

The solutions are of the type

$$N_+(t) = A \exp(-t/\tau_{\text{short}}) + B \exp(-t/\tau_{\text{long}}) \quad (8)$$

Thus, the simple two-chamber model predicts the decay of the impurity content with two time constants, where

$$\frac{1}{\tau_{\text{short}}} = \frac{1}{2\tau} \left(1 + \sqrt{1 - \frac{4\tau^2}{\tau_p \tau_{\text{pump}}}} \right) \quad (9)$$

$$\frac{1}{\tau_{\text{long}}} = \frac{1}{2\tau} \left(1 - \sqrt{1 - \frac{4\tau^2}{\tau_p \tau_{\text{pump}}}} \right) \quad (10)$$

with

$$\frac{1}{\tau} = \frac{1}{\tau_p} + \frac{\gamma}{\tau_D} + \frac{1}{\tau_{\text{pump}}} \quad (11)$$

These predictions will be compared with experimental results in Section 3. For the unknown quantities it follows from Eqs (9–11) that

$$\tau_{\text{pump}} = \frac{\tau_{\text{short}} \tau_{\text{long}}}{\tau_p} \quad (12)$$

$$\frac{\tau_D}{\gamma} = \frac{\tau_{\text{short}} \tau_{\text{long}} \tau_{\text{pump}}}{(\tau_{\text{pump}} - \tau_{\text{short}})(\tau_{\text{long}} - \tau_{\text{pump}})} \quad (13)$$

2.2. Scaling laws for τ_D

For the dependence of the divertor retention capability on divertor plasma parameters (n_e , T_e) and on the impurity species, further predictions can be made. If neutral gas flow from the divertor to the main plasma is the dominant recycling path, the time constant τ_D/γ will depend on the ionization length of recycling impurities in relation to the dimensions of the divertor plasma. The ionization length is given by

$$\lambda_{\text{ion}} = \frac{v_0}{n_e S_{\text{ion}}(T_e)} \quad (14)$$

where v_0 is the thermal velocity of the recycling gas and S_{ion} is the ionization rate coefficient for impurity atoms. Evidently, recycling by neutral backflow will become less probable, i.e. τ_D will become longer, as the divertor density and temperature increase and as the impurity mass, which determines v_0 , increases. For low divertor temperatures and long ionization lengths the divertor retention time constant is ultimately equal to the vacuum time constant of the divertor entrance slits [20, 25].

For the case of high divertor temperatures the ionization length becomes so small that neutral backflow is no longer of importance. In this case the retention of impurity ions has to be considered. The characteristic decay length λ_{\parallel} of the impurity density along field lines can be obtained in stationary conditions from a balance of the pressure gradient dP_z/ds and friction terms [13, 26].

The decay length λ_{\parallel} is thereby given by the ratio of the diffusion coefficient along field lines, D_{\parallel} , to the velocity of the background plasma, v_{\parallel} . The background plasma streams towards the divertor plates with a Mach number M [27].

$$\lambda_{\parallel} [\text{m}] = \frac{D_{\parallel}}{v_{\parallel}} \approx \frac{8.84 \times 10^{16} T_i^2 [\text{eV}]}{\left(1 + \frac{m_i}{m_z}\right) \ln \Lambda M Z^2 n_i [\text{m}^{-3}]} \quad (15)$$

where $\ln \Lambda$ is the Coulomb logarithm (typically 15 to 18) and Z is the charge state of the impurity ions. This characteristic length has now to be compared with the connection length of the field lines from the divertor plates to the X-point, and the residence probability for impurities in the main plasma is given by

$$P \propto \exp(-L_{\parallel}/\lambda_{\parallel}) \quad (16)$$

In reality, parameters such as thermal drag forces, which depend on the gradient of T_i , have to be taken into account. This simplified consideration may,

however, help to understand the importance of the divertor ion temperature and density. The dependence of λ_{\parallel} on the divertor plasma parameters shows that for high ion temperature and consequently low density, the retention of ionized impurities may break down. Thus, a minimum divertor temperature is required for the retention of neutral atoms, whereas there is a maximum divertor temperature for the retention of ions. Additionally, the retention of ions depends critically on the ion charge state Z . More quantitative estimates will be given in the discussion of experimental values for different impurity species.

2.3. 1-D transport code calculations

The two-chamber model outlined above can give good insight into the expected time dependences and stationary values. The extraction of the divertor retention time τ_D/γ from the experimental decay of impurities after a gas puff is, however, often highly uncertain. In Eq. (13) the difference $\tau_{\text{long}} - \tau_{\text{pump}}$ is given in the denominator. This difference may become small and the determination of τ_{pump} from Eq. (12) may often not be precise enough, in particular because of uncertainties in the determination of τ_p . Therefore, values of τ_D and γ are better obtained by fully time dependent 1-D impurity transport code simulations of the different impurity line intensities in the main plasma after short gas puffs. The code ZEDIFF [21] had been modified to allow for recycling of neutral gas from the divertor [5]. Input parameters for the code are the experimentally determined $n_e(r)$ and $T_e(r)$ profiles, the cross-field diffusion coefficient D_{\perp} , the inward drift velocity v_{in} , the mean energy of the neutral source atoms E_0 and

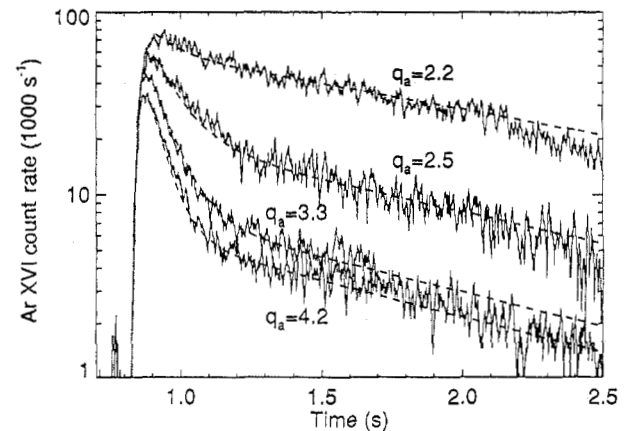


FIG. 2. Temporal decay of the Ar XVI line after Ar injection in Ohmic discharges.

the time constant τ_{\parallel} for losses parallel to the magnetic field lines outside the separatrix. These parameters determine the boundary shielding (γ) for thermal gaseous impurities as well as the impurity concentration profile inside the plasma separatrix. The values obtained for γ enable a comparison of τ_D from the transport code with τ_D/γ obtained from the two-chamber model. Main further output parameters from ZEDIFF are the traces of selected line intensities that can be compared with experimental data, the impurity content in the main plasma and the global impurity confinement time τ_p . The fitting parameters to experimental data are the divertor retention time constant τ_D and the pumping time constant τ_{pump} .

3. RESULTS

3.1. Dependence of τ_D on the safety factor q

In ASDEX, the divertor retention was investigated extensively for inert gases. Short gas puffs were applied in the main chamber and the decay of the impurity line radiation in the main plasma was monitored. Figure 2 shows the temporal decay of the Ar XVI line after Ar injection into the Ohmic phase of discharges with various values of the safety factor q ($I_p = \text{const}$). Two exponential decay times are clearly seen, as predicted by the two-chamber model. The fast decay includes the outflux from the plasma into the divertor until equilibrium is established. The slow decay includes mainly the effect of Ar pumping through the divertor chambers by external pumps. This is in contrast to results from JET [8], where no Ar pumping could be detected, since the external pumps are far from the X-point position. The pumping time constant in ASDEX is found to be $\tau_{\text{pump}} \approx 1$ s from Eq. (12), taking into account that τ_p will be close to τ_{short} . A precise determination of τ_D from Eq. (13) is not possible since, with τ_p close to τ_{short} , τ_{pump} will be close to τ_{long} . However, the fact that the relative contribution of the fast decay decreases with q indicates clearly a decrease of the divertor retention capability.

To avoid the uncertainties resulting from the analytical formulation, the spectroscopic data have been fitted using the transport code ZEDIFF (see Section 2.3), and the resulting values of τ_D are given in Table I. The diffusion coefficient D_{\perp} and the inward drift velocity v_{in} determine the particle confinement time τ_p , which is also included in Table I. Taking these values, $N_+(t)$ was calculated for the two-chamber model from Eq. (8), and the obtained fit to the time dependence is

TABLE I. VALUES OF τ_p AND τ_D IN OHMIC ASDEX DIVERTOR DISCHARGES FOR DIFFERENT SAFETY FACTORS q_a ($\tau_{\text{pump}} = 1$ s)

q_a	τ_p (ms)	τ_D (ms)
4.2	65	700
3.3	95	650
2.5	130	550
2.16	150	300

shown in Fig. 2 (dashed lines). In particular, for $q < 3$, a drastic reduction of the divertor confinement occurs. For $q = 2.16$, the obtained values are highly uncertain, though the same trend clearly continues. The values given in Table I show an increase of τ_p and a decrease of τ_D with decreasing q . The increase of τ_p is obvious from the change of τ_{short} in Fig. 2. This increase of τ_p has been observed earlier in ASDEX during laser blow-off investigations with Ti [28] and modulated impurity gas puffing [29, 30] with H_2S and HBr . The decrease of τ_D with q can be understood by the corresponding decrease of the connection length L_{\parallel} along field lines from the divertor plates to the X-point. This indicates that ionic impurity transport dominates in this operational regime. L_{\parallel} increases from 1.3 m at $q = 2.2$ to 2.8 m at $q = 4.2$. However, taking the typical divertor parameters, i.e. $T_e = 13$ eV and $n_e = 1 \times 10^{19} \text{ m}^{-3}$ independent of q , and $T_e = T_i$ and $M = 0.1$, a much stronger dependence on q would be expected from Eq. (16). Assuming lower Mach numbers ($M = 0.02$), a weaker dependence on q , i.e. better agreement with the experimental data, is obtained. This will be discussed in more detail in the next section on the dependence of τ_D on auxiliary heating power, for which more information exists on the divertor plasma parameters.

3.2. Dependence of τ_D on auxiliary heating power (NBI)

Whenever the ionic impurity transport dominates over neutral recycling, an additional increase of the divertor temperature will make the divertor plasma more transparent for ions, according to Eq. (15). Thus, for additional heating, a decrease of the divertor retention can be expected. This was actually observed in ASDEX [5, 12], DIII-D [9] and JET [8]. For these three machines the same computer code, ZEDIFF, was used for a fully time dependent evaluation of the divertor retention and pumping time constants. A compari-

TABLE II. COMPARISON OF τ_D AND τ_{pump} FOR DIVERTOR DISCHARGES WITH AND WITHOUT NBI*

		DIII-D		ASDEX		JET	
		τ_D	τ_{pump}	τ_D	τ_{pump}	τ_D	τ_{pump}
Ar	Ohmic	130	1000	300	950	<400	∞
	NBI	70	1000	see Table III		<400	∞
He	Ohmic			100		300	∞
	NBI			40		150	∞

* The values of τ_D and τ_{pump} are given in milliseconds.

TABLE III. DEPENDENCE OF τ_D ON THE NBI POWER FOR ASDEX DIVERTOR DISCHARGES*

P_{NBI} (MW)	n_e (10^{19} m^{-3})	T_e (eV)	τ_D (ms)
0.0			320
0.3	1.3	11	320
0.6	1.65	16	220
1.2	1.65	19	130
1.8	1.7	21.5	90
3.4	1.5	20	20

* The values in the last row are from Ref. [5].

son of values for τ_D and τ_{pump} with and without NBI is given in Table II. Compared to DIII-D and JET, the closed divertor of ASDEX has high values of τ_D . Since for impurity retention the value τ_D/γ is relevant, the larger machines may still have better impurity retention owing to improved boundary shielding. For all three machines, τ_D deteriorates during NBI. In JET discharges where Xe was added to the working gas, the edge and X-point cooling due to radiation led to the highest divertor confinement time constants [8].

The dependence of τ_D on NBI power is given in Table III for the case of ASDEX. For low NBI power the Ar XVI line intensity decreases compared to the Ohmic level, as expected, without a change of τ_D ; this is due to the outward shift of the radiating shell of Ar XVI. For increased NBI power an increase of the AR XVI intensity is observed, indicating enhanced backflow of argon from the divertor which is due to a breakdown of the divertor retention. In Table III, the

divertor retention time constants are given together with the divertor plasma parameters n_e and T_e .

The data from Table III for ASDEX are plotted in Fig. 3 as a function of NBI power, together with similar data from DIII-D. Also introduced are normalized values for τ_D as expected from Eqs (15) and (16), taking a connection length L of 2 m, an ion charge state $Z = 2$ and a Mach number of 0.1, and assuming $n_i = n_e$ and $T_i = T_e$. It is evident that with these assumptions a much stronger decrease of τ_D would be expected. If, however, a Mach number of only 0.015 is used, a reasonably good scaling can be obtained. Such a low Mach number was obtained from 1-D fluid calculations [13, 14] close to the divertor throat.

Figure 3 shows clearly that for Ohmic heating or for moderate NBI the divertor temperatures are low, and the impurity ions are retained in the divertor by friction with the streaming background plasma. τ_D values considerably higher than the vacuum time constant for neutral gas [25] are obtained. As the temperature increases, λ_{\parallel} increases in proportion to T_i^2 and, eventually, the plasma pumps ionized impurities more efficiently along field lines than neutral gas streams through the divertor throat. The high temperature limit of τ_D is only a fraction of the vacuum time constant, which was determined to be about 90 ms [25].

3.3. Dependence of τ_D on central plasma density

The divertor retention for non-recycling impurities, such as Cu produced at the divertor plates, was shown to be a strong function of the line averaged plasma

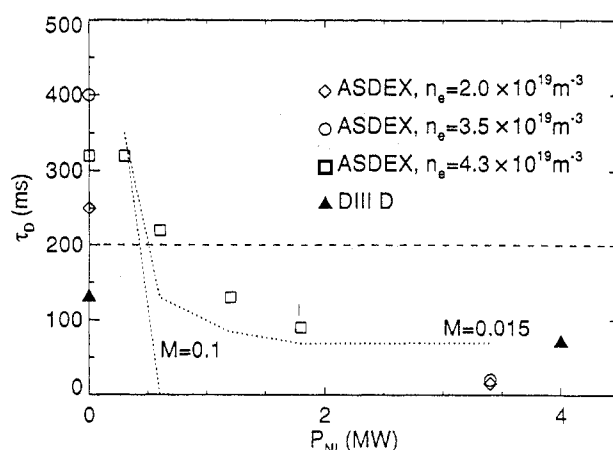


FIG. 3. Dependence of τ_D on the NBI power. The dotted lines are calculated from Eqs (15) and (16) for different Mach numbers M . The dashed line indicates the vacuum time constant of the divertor throat for Ar.

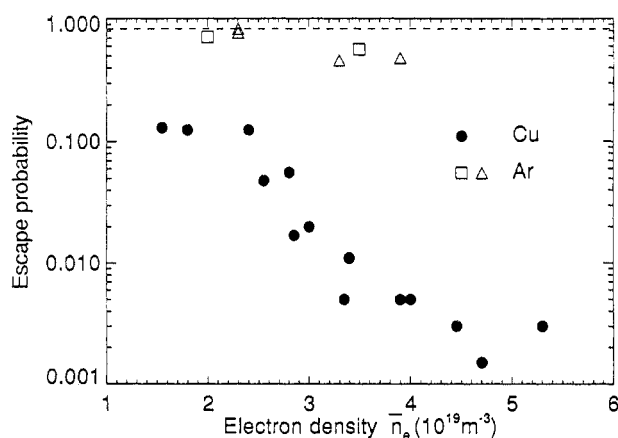


FIG. 4. Dependence of the escape probabilities of non-recycling impurities (Cu) [12] and recycling impurities (Ar) from the divertor on the line averaged plasma density \bar{n}_e in Ohmic discharges. The triangles denote data determined by mass spectrometry and the squares denote data obtained from spectroscopic measurements. The dashed line indicates the estimated escape probability due to the vacuum time constant of the divertor throat.

density \bar{n}_e [12]. With increasing \bar{n}_e , the divertor density n_e increases, while T_e decreases. Going from $\bar{n}_e = 2 \times 10^{19} \text{ m}^{-3}$ to $\bar{n}_e = 5 \times 10^{19} \text{ m}^{-3}$, the retention factor for Cu increases by a factor of more than 40 for Ohmic discharges.

When the global confinement time for Cu atoms eroded at the divertor plates (as determined experimentally in Ref. [12]) is divided by the plasma particle confinement time τ_p , the escape probability of Cu atoms from the divertor can be obtained. This escape probability is shown in Fig. 4 as a function of the line averaged plasma density.

For Ar, the dependence of the divertor retention time on the central plasma density was reported earlier [5, 25]. In contrast to Cu, an improvement of only about a factor of two was found, with τ_D remaining close to the vacuum time constant for the divertor duct. To compare recycling and non-recycling impurities also for Ar, the escape probability from the divertor to the main plasma can be obtained when τ_D and τ_{pump} are known. The corresponding escape probability is also given in Fig. 4. The expected difference between non-recycling and recycling impurities is clearly seen, both in the absolute values of the escape probability and in the decrease towards higher plasma densities.

Recycling impurities, however, may hit the walls of the divertor throat, be neutralized and make another attempt to escape. Thus, the decrease of τ_D with increasing \bar{n}_e is not expected to be as drastic as for

non-recycling impurities, and values not differing much from the vacuum time constant for the divertor throat are expected. τ_D improves from 250 ms to 400 ms during OH and from 15 ms to 20 ms for NBI for $\bar{n}_e = 2 \times 10^{19}$ to $\bar{n}_e = 3.5 \times 10^{19} \text{ m}^{-3}$ [5]. Very similar values have been obtained by Ar puffing into one divertor chamber and measuring the partial pressure of Ar in the opposite divertor chamber [25]. As the divertor density n_e increases almost linearly with \bar{n}_e while the divertor temperature T_e decreases, such a scaling of τ_D is in good agreement with Eqs (14) and (15).

3.4. Dependence of τ_D on impurity species

To allow scaling of heavy inert gases to He^{2+} particles produced in fusion processes, it is necessary to use different inert gas pulses in otherwise similar plasma conditions. Actually, both Eq. (15) and Eq. (16) contain parameters relevant to the impurity species, such as the thermal velocity v_0 of the impurities or their mass m_z . For Ohmic ASDEX discharges with a relatively low NBI power of 0.7 MW, the dependence of the He II, Ne VII and Ar XVI line intensities is shown in Fig. 5. The equivalent gas puff was applied in the Ohmic phase at a time of 0.8 s and the NBI was turned on at 1.7 s. For the heavy inert gases Ar and Ne, the observed decrease of the line intensity is even stronger than expected from the changed temperature and density profiles in the main plasma alone. Only small changes of τ_D are deduced for this low neutral injection level. For He, however, the line intensity of

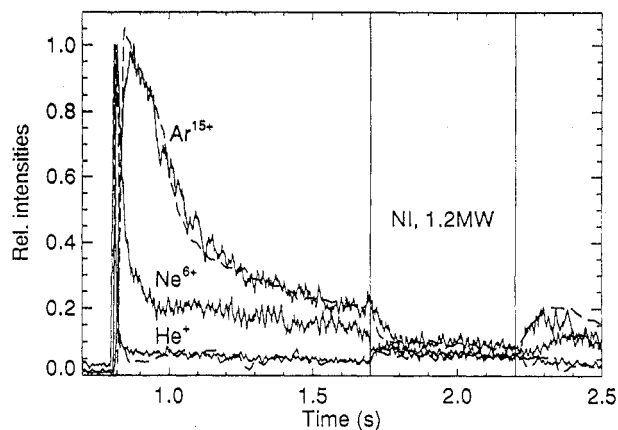


FIG. 5. Time dependence of the line radiation of different impurity species in Ohmic ASDEX discharges. The dashed lines are results from transport code simulations used to determine τ_D in the OH and NBI phases, respectively.

TABLE IV. VALUES OF τ_D (in ms) FOR HELIUM, NEON AND ARGON FOR OH AND NBI PLASMA PHASES

	He	Ne	Ar
OH	100	120	250
NBI	40	80	250

Gas	T_e	5 eV	10 eV	20 eV	50 eV	100 eV
He		180	10	1.9	0.53	0.4
				12.5	80	320
Ne		39	2.8	0.5	0.15	0.08
			2.8	17.4	109	436
Ar		1	0.15	0.05		
			5	20	123	331

* The ionization length λ_{ion} (left upper corner) from Eq. (14) and the parallel decay length $\lambda_{||}$ (right lower corner) from Eq. (15) are given for divertor plasmas of $n_e = 1 \times 10^{19} \text{ m}^{-3}$ and various values of T_e . The dotted areas indicate regimes of poor divertor confinement.

He II increases, indicating a strong decrease of divertor confinement. The values of τ_D for He, Ne and Ar as obtained from fits using the ZEDIFF code for Ohmic and NBI phases ($P_{NI} = 0.7 \text{ MW}$) are given in Table IV. For divertor parameters estimated as $n_e = 1 \times 10^{19} \text{ m}^{-3}$ and $T_e = 10 \text{ eV}$, the ionization length for He is still larger than the divertor plasma extensions, while the calculated ionization lengths for Ar and Ne are much shorter. In Table V, the ionization lengths λ_{ion} for He, Ne and Ar obtained from Eq. (15) are listed for various divertor temperatures T_e ; the dotted areas indicate regimes of poor confinement due to inadequate ionization. Also included in Table V are the ion density decay lengths $\lambda_{||}$ parallel to the magnetic field lines obtained from Eq. (16) for an assumed Mach number of 0.015. The dotted areas show regimes of long decay length compared to a connection length of 200 cm to the X-point. Thus, Table V shows that both low and high divertor temperatures lead to poor divertor retention. There is only a narrow window for good He retention, at least for the ASDEX divertor geometry, around $T_e = 20 \text{ eV}$.

4. CONSEQUENCES FOR HELIUM EXHAUST

The retention capabilities of different divertor or pumped limiter geometries will be evaluated for the case of a steady state α -particle production rate in a central burning plasma. The α -particle content in the main plasma is given by Eq. (6), from which the effective He confinement time is derived as

$$\tau_{eff} = \left(1 + \gamma \frac{\tau_{pump}}{\tau_D}\right) \tau_p \quad (17)$$

This is equivalent to an equation derived in Ref. [4] where $\gamma \tau_{pump}/\tau_D$ was replaced by $1/\epsilon_p$. The exhaust efficiency of a pumping system was defined through ϵ_p

$$\Phi_{pump} = \epsilon_p \Phi_+ \quad (18)$$

Thus, within the present description of the exhaust system, the central impurity content N_+ , which is determined by α -particle confinement as $N_+ = Q_+ \tau_p$ for non-recycling impurities [3, 4], will be enhanced by the factor $E = 1 + \gamma \tau_{pump}/\tau_D$ in the case of recycling impurities. Therefore, an exhaust system must provide not only good retention through a long τ_D but also an adequate pumping of impurities through a short τ_{pump} .

We have seen from Table II that for the three divertor experiments the divertor retention times are within a narrow range, 130–400 ms, for OH conditions. A change from the closed divertor configuration in ASDEX to the widely open X-point geometry in JET, which has no proper divertor plasma, showed surprisingly little influence on τ_D . This may be due to the fact that the ionization lengths for recycling neutrals in all three cases are short compared to the dimensions of the divertor fan, and neutral recycling can be neglected. The boundary shielding obtained from the code simulations is also similar for the three experiments, yielding a fraction γ of only about 10% of the recycling flux entering the confined plasma. However, the pumping time constant is widely different. While for a pumped divertor the typical values of the pumping time for DIII-D and ASDEX are around 1 s, pumping through the main vessel leads to extremely long pumping times in JET.

Assuming that for a pumped divertor a pumping time constant of 1 s can be obtained, the enhancement factor E ranges between 1.2 and 2. For pumped limiter conditions, shorter pumping time constants can be achieved generally [10, 11]. On the other hand, the shielding efficiency of the boundary layer may not be as good as was assumed; this is due to the recycling close to the separatrix of the confined plasma [31]. Thus, achievable values for ϵ_p of the order of only

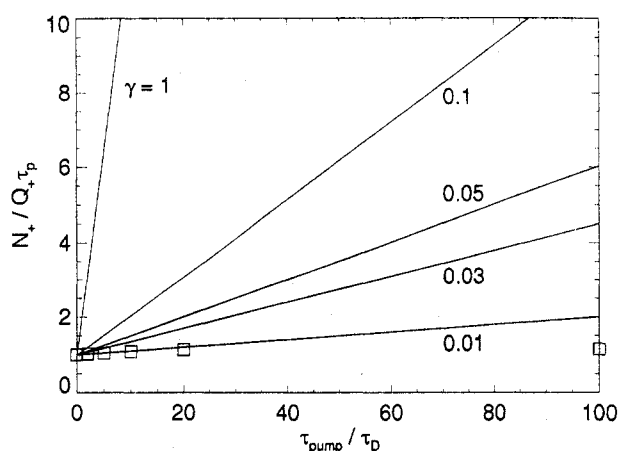


FIG. 6. Particle number in the plasma normalized by the α -particle production during one confinement time τ_p versus $\tau_{\text{pump}}/\tau_D$ for different values of γ . The squares are results from transport code simulations.

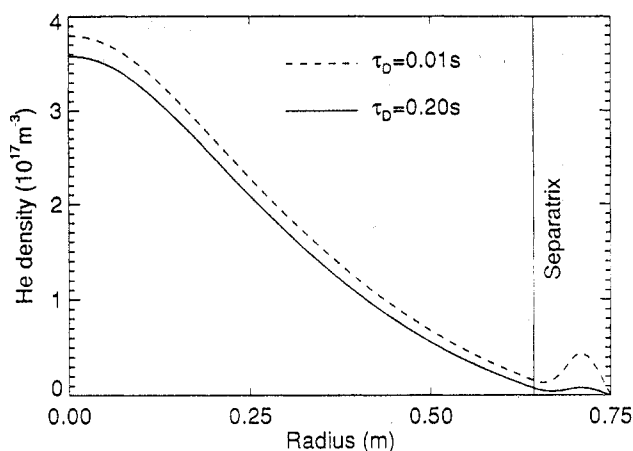


FIG. 7. Radial profile of the He density for different divertor retention time constants τ_D (calculated with plasma parameters of an Ohmic discharge in DIII-D).

10% were reported [32], yielding an enhancement factor of about 10.

One further consideration must be made regarding the different confinement times τ_p and $\gamma\tau_p$. As already discussed in Section 2, the confinement time of centrally produced α -particles after thermalization is expected to be much longer than the global confinement time of recycling He atoms entering the plasma through the boundary layer. If one calculates the central He content normalized by the α -particle production during one confinement time, $N_+/Q_+\tau_p$, one obtains from Eq. (6) a dependence on $\gamma\tau_{\text{pump}}/\tau_D$. This value is shown in Fig. 6 for different values of the parameter γ . Already for $\gamma = 1$, enhancement factors

of 10, as expected for pumped limiters, will drastically increase the He content. For smaller values of γ , the relative enhancement due to recycling will be less pronounced. Actually, code calculations for the case of DIII-D, assuming D-T plasmas with central parameters $\bar{n}_e = 1.2 \times 10^{20} \text{ m}^{-3}$ and $T_e = 20 \text{ keV}$, resulted in values of γ smaller than 0.01 [9]. The central He content obtained from the calculations is introduced in Fig. 6 and indeed lies close to that from model calculations for $\gamma = 0.01$.

The effect of a wide variation of $\tau_{\text{pump}}/\tau_D$ on the He profile can be seen in Fig. 7, again for the geometry and confinement parameters of Ohmic discharges in DIII-D. For cases where $\tau_{\text{pump}}/\tau_D = 5$, i.e. a situation found in today's divertor tokamaks, recycling He atoms led to a small increase of the He concentration near the separatrix. Even for cases where $\tau_{\text{pump}}/\tau_D = 100$, i.e. for pumping time constants higher by a factor of 20 than those observed, recycling increases the He concentration only in the boundary layer while the central He concentration is only slightly enhanced. For both cases, the He concentrations are of the order of 0.2%.

5. CONCLUSIONS

In spite of the complicated nature of impurity recycling from divertors to the main plasma, a simple global time constant τ_D together with the boundary shielding efficiency γ can be used to describe this effect of recycling. This time constant can be obtained from the time dependent impurity line radiation after short pulse injection. It is a useful quantity in comparisons of different divertor geometries and of the dependences on plasma density and auxiliary heating.

Experimental determination of the divertor retention for fully recycling impurities shows that an increase of the divertor plasma temperature drastically reduces the retention efficiency. This indicates that for today's divertor experiments the recycling of impurities from the divertor is predominantly ionic in nature. To retain the He ions in the divertor, the ion temperature should not exceed 20 eV. Higher ion temperatures may be acceptable only at correspondingly higher ion densities. However, for a much lower electron temperature the long ionization lengths may lead to enhanced neutral backflow to the main plasma.

The geometry of the divertor does not strongly influence its retention capability. Similar retention time constants are found for the closed ASDEX divertor chamber, the open divertor of DIII-D and the JET

X-point geometry. The additional influence of the boundary shielding leads to better impurity retention in the larger machines.

To achieve adequate He removal rates, the pumping has to be done through the divertors. For JET conditions, i.e. pumping at the vessel midplane, extremely large pumping time constants are found.

The advantage of a divertor over a pumped limiter, as far as He retention is concerned, lies in the higher plasma boundary shielding for recycling He atoms in a divertor. The pumping time constant may be lower for limiters, but it is still adequate for today's divertor geometries.

The He content in the main plasma is still dominated by the production rate times the central He confinement time, Q_+/ τ_p . Divertors or pumped limiters only can keep the enhancement of the He content due to recycling low and provide limited volumes of enhanced neutral gas pressure for improved pumping. Divertors, however, ensure a good retention capability for divertor produced non-recycling impurities.

REFERENCES

- [1] The JET Team (presented by M. Keilhacker), *Plasma Phys. Control. Fusion* **33** (1991) 1453.
- [2] The JET Team (presented by P.R. Thomas), *J. Nucl. Mater.* **176&177** (1990) 3.
- [3] BEHRISCH, R., PROZESKY, V., *Nucl. Fusion* **30** (1990) 2166.
- [4] REITER, D., WOLF, G.H., KEVER, H., *Nucl. Fusion* **30** (1990) 2141.
- [5] JANESCHITZ, G., FUSSMANN, G., KOTZE, P.B., et al., *Nucl. Fusion* **26** (1986) 1725.
- [6] NEUHAUSER, J., ARATARI, R., BESSENRODT-WEBERPALS, M., et al., in *Plasma Physics and Controlled Nuclear Fusion Research 1990* (Proc. 13th Int. Conf. Washington, DC, 1990), Vol. 1, IAEA, Vienna (1991) 365.
- [7] JANESCHITZ, G., GIANELLA, R., JAECKEL, H.J., et al., in *Controlled Fusion and Plasma Heating* (Proc. 17th Eur. Conf. Amsterdam, 1990), Vol. 14B, Part III, European Physical Society (1990) 1365.
- [8] JANESCHITZ, G., GOTTARDI, N., JAECKEL, H., et al., in *Controlled Fusion and Plasma Physics* (Proc. 18th Eur. Conf. Berlin, 1991), Vol. 15C, Part III, European Physical Society (1991) 97.
- [9] LIPPMANN, S., MAHDAVI, A., ROTH, J., KRIEGER, K., FUSSMANN, G., JANESCHITZ, G., *ibid.*, p. 201.
- [10] HILLIS, D.L., DIPPEL, K.H., FINKEN, K.H., et al., *Phys. Rev. Lett.* **65** (1990) 2382.
- [11] FINKEN, K.H., DIPPEL, K.H., HARDTKE, A., et al., *J. Nucl. Mater.* **176&177** (1990) 816.
- [12] ROTH, J., JANESCHITZ, G., *Nucl. Fusion* **29** (1989) 915.
- [13] NEUHAUSER, J., SCHNEIDER, W., WUNDERLICH, R., LACKNER, K., *Nucl. Fusion* **24** (1984) 39.
- [14] NEUHAUSER, J., SCHNEIDER, W., WUNDERLICH, R., LACKNER, K., *J. Nucl. Mater.* **121** (1984) 194.
- [15] NEUHAUSER, J., BRAAMS, B., KRECH, M., RITSCHEL, U., SCHNEIDER, W., WUNDERLICH, R., *Contrib. Plasma Phys.* **30** (1990) 95.
- [16] NEUHAUSER, J., "Radiation control in poloidal divertor tokamaks", in *Relevance, Realization and Stability of a Cold Layer at the Plasma Edge for Fusion Reactors* (Proc. Satellite Workshop of 9th Int. Conf. on Plasma Surface Interactions, Castle of Cadarache, 1990), Rep. DRFC/CAD EUR-CEA-FC-1403, CEA, Centre d'études de Cadarache, Association Euratom-CEA, Saint Paul-lez-Durance (1990) 243.
- [17] NEUHAUSER, J., BESSENRODT-WEBERPALS, M., BRAAMS, B.J., et al., *Plasma Phys. Control. Fusion* **31** (1989) 1551.
- [18] BROOKS, J.N., *Phys. Fluids B* **2** (1990) 1858.
- [19] BROOKS, J.N., *J. Nucl. Mater.* **170** (1990) 164.
- [20] FUSSMANN, G., POSCHENRIEDER, W., BERNHARDI, K., RICHTER, B., SZYMANSKY, Z., and ASDEX Team, *J. Nucl. Mater.* **121** (1984) 164.
- [21] JANESCHITZ, G., RAN, L.B., FUSSMANN, G., KRIEGER, K., STEUER, K.H., and ASDEX Team, Determination of Impurity Concentrations and of Z_{eff} by VUV Spectroscopy on ASDEX, Rep. IPP III/147, Max-Planck-Institut für Plasmaphysik, Garching (1990).
- [22] BRAAMS, B.J., IPP Annual Report 1986, Max-Planck-Institut für Plasmaphysik, Garching (1987) 28.
- [23] BRAAMS, B.J., A Multi-fluid Code for Simulation of the Edge Plasma in Tokamaks, Tech. Rep. EUR-FU/XII-80/87/68, NET Team, Garching (1987).
- [24] FUSSMANN, G., *Nucl. Fusion* **26** (1986) 983.
- [25] POSCHENRIEDER, W., *J. Vac. Sci. Technol., A* **5** (1985) 2265.
- [26] NEUHAUSER, J., WUNDERLICH, R., *J. Nucl. Mater.* **145-147** (1987) 877.
- [27] FUSSMANN, G., *Plasma Phys. Control. Fusion* **32** (1990) 662 (Conf. Rep.).
- [28] SETZENSACK, C., Laser-blow-off-Experimente am ASDEX, Rep. IPP-III/119, Max-Planck-Institut für Plasmaphysik, Garching (1987).
- [29] KRIEGER, K., FUSSMANN, G., ASDEX Team, *Nucl. Fusion* **30** (1990) 2392.
- [30] KRIEGER, K., FUSSMANN, G., in *Controlled Fusion and Plasma Heating* (Proc. 17th Eur. Conf. Amsterdam, 1990), Vol. 14B, Part III, European Physical Society (1990) 1431.
- [31] MADDISON, G.P., BAELEMAN, T., BÖRNER, P., HOTSTON, E.S., REITER, D., in *Controlled Fusion and Plasma Physics* (Proc. 18th Eur. Conf. Berlin, 1991), Vol. 15C, Part III, European Physical Society (1991) 197.
- [32] DIPPEL, K.-H., FINKEN, K.-H., HARDTKE, A., et al., in *Plasma Physics and Controlled Nuclear Fusion Research 1988* (Proc. 12th Int. Conf. Nice, 1988), Vol. 1, IAEA, Vienna (1989) 453.

(Manuscript received 18 May 1992)

Final manuscript received 5 August 1992)